Results in Engineering 21 (2024) 101735

Contents lists available at ScienceDirect

Results in Engineering

journal homepage: www.sciencedirect.com/journal/results-in-engineering

Reliability assessment of carbon fiber mortar: Combined pulse velocity, point load, and compressive strength tests

Achmad Bakri Muhiddin [a,*], M.W. Tjaronge [a], Muhammad Akbar Caronge [a], Nur Hafizah A. Khalid [b]

[a] Department of Civil Engineering, Faculty of Engineering, Universitas Hasanuddin, Gowa, 92171, Indonesia
[b] Faculty of Civil Engineering, Centre for Advanced Composite Materials, Universiti Teknologi Malaysia, 81310, Johor Bahru, Johor, Malaysia

ARTICLE INFO

Keywords:
Pulse velocity
Point load
Compressive strength
Carbon fiber
Mortar

ABSTRACT

Cement mortar is used as an adhesive and plaster for brick walls, drainage channels or irrigation with river stones or mountain stones, and in the manufacturing of short revetments. The performance of cement mortar requires continuous improvement by construction materials researchers, scientists, and building contractors. Recently, carbon fiber sheet has gained popularity for use in retrofitting and improvement to the performance of building elements. This study aims to recycle small sheets of unused carbon fiber by cutting them into short carbon fiber (SCF) with a uniform length of 12 mm, which is used as an internal reinforcement in the cement mortar. All plain and fibrous mortar were prepared with a 50 mm cube mold. In addition, tests were conducted to provide reliable data regarding the application of recycled carbon fiber sheets as discrete fiber reinforcement in the improvement of cement mortar; these include ultrasonic pulse velocity (UPV), compressive strength, and point load strength index (PLSI) (known for performance rock testing in geotechnical and geological environments) tests. The test results for UPV, PLSI, and compressive strength showed that the addition of carbon fiber improves the performance of the mortar when compared to plain mortar. Furthermore, two simplified relationships are made: the first correlation was for PLSI with compressive strength, and the second correlation was for UPV with compressive strength. Finally, these correlations were compared with those of experimental tests obtained from published literature, thus demonstrating the correctness of the PLSI, compressive strength, and UPV values obtained in this study.

1. Introduction

Cement mortar has been used for a variety of constructions. These include brick binders for the walls of houses and buildings, fences, drains, retaining walls, etc. Owing to their widespread use, civil engineers continue to improve the performance of cement mortar and aim to make it an affordable easy-to-apply construction material. Researchers have proposed employing numerous types of fibers to improve the performance of cementitious composites [1]. Among them is carbon fiber reinforced polymer (CFRP). CFRP is a type of composite materials produced from carbon fiber reinforcement and resin. CFRP possesses several advantages, such as exceptional strength, stiffness, low density, and resistance to corrosion, as a result, various industrial sectors, particularly aerospace, automotive and construction, extensively utilize CFRP in numerous applications. Simultaneously, the amount of CFRP waste increased significantly, gaining approximately 4 million tons globally in 2017 [2]. Furthermore, it is estimated that at least 26,000 tons of discarded CFRP products will be disposed in landfills every year in 2020. Nevertheless, the CFRP decomposition process in landfills is very slow at only 1 % of the original mass weight over a 100 year. Consequently, it is crucial to find innovative ways for dealing with these wastes and reduce their negative effects to the surrounding environment [3].

CFRP as an advanced building material has been widely produced in the form of continuous carbon fiber sheets and discrete short carbon fiber with specified designations. Currently, continuous carbon fiber sheet as an advanced material for strengthening and repairing structural elements is widely recognized [4–8]. However, there are unused carbon fiber sheets in the form of small sheets or rags resulting from large-scale construction projects. Owing to carbon fiber sheets being very difficult to decompose in nature, it is necessary to recycle unused small pieces to limit the negative effects on the storage location. However, an

* Corresponding author.
E-mail address: bakrim@unhas.ac.id (A.B. Muhiddin).

https://doi.org/10.1016/j.rineng.2023.101735
Received 1 October 2023; Received in revised form 16 December 2023; Accepted 29 December 2023
Available online 30 December 2023

interesting alternative that has a positive economic and environmental impact is to recycle small sheets of unused carbon fiber into short-cut carbon fiber (SCF). The SCF derived from unused carbon fiber sheets may be comparable to the virgin short carbon fiber; hence, it can be used as a valuable construction material. It is widely established that short fibers improve the mechanical nature of mortars by providing superior crack bridging ability and good bond strength to the cement matrix. In current years, short fibers have been used effectively to improve the mechanical characteristics of cement-based materials like concrete [9,10], mortar [11,12], and ECC [13–15]. Based on many experimental campaigns, there has been a widespread consensus that related basalt [16–18], polypropylene [19–21], polyvinyl alcohol [22], steel [23,24], glass [25–27], and carbon fibers [28–30] improve the tensile properties, flexural properties, and durability of mortar.

In the last decades, knowledge regarding the mechanism of short-cut carbon fiber has advanced tremendously to improve the mechanical properties of cement-based materials, such as mortar [31]. However, excessive amounts of short fibers including carbon fiber will impede uniform dispersion, and cause balling by producing internal flaws that impair the structural integrity of the hardened mortar [32]. Thus, the recommended amount addition of SCF is 0.25–0.8 % by volume mixture or 1.25–6.48 % of weight of binder [1,2,33]. Saccani et al. [34] studied SCF coated by the resin having 5–8 mm in length at dosages 1 %–4.5 % of volume on mechanical properties of Portland cement (PC) and geopolymer (GP) composite. It is found that compressive strength is barely affected by SCF in all composite system. But flexural strength improved by about 20 % in both PC and GP systems compared to without SCF. Nguyen et al. [35] examined the use of CFRP waste with dimensions of 3–6 mm and at amount of 2–3 % weight of cement as a reinforcing material in cement composites. Their observation shows notable improvements of 10–15 % and 15–25 % in the compressive and flexural bending strengths, respectively, in addition to enhanced resistance to fracture. Belli et al. [36] reported that compressive strength of SCF mortar is higher about 10–27 % than reference mortar by adding 0.4–0.8 % SCF by volume. Further, flexural and split tensile strengths of mortar composite with 0.4–0.8 % SCF improved by up to 200 % and 190 %, respectively. During the loading process, the presence of SCF in an optimal amount inhibits crack growth and bridges across the formed microcracks. Consequently, a larger load in terms of indirect tensile stress [37], direct (uniaxial) tensile stress [38–40], flexural stress [37–41], and compressive stress [41] is required to cause the damage that develops macro cracks. With the advantages possessed by SCF as a reinforcing material in cementitious system, SCF mixture applications are widely used in industrial flooring, precast concrete, shotcrete or sprayed concrete, tunnel linings, slope protection and etc., [42].

The ultrasonic pulse velocity (UPV) test has been widely recognized as a valuable non-destructive test that provides great advantages. It can be performed with less time, simple operation, and can be conducted in the field and laboratory. The UPV value that refers to the *P* wave velocity is one of the important physical properties used in characterizing the solid material such as rocks, cement-based materials (concrete), mortar, and paste cemented backfill. The basic concept of the UPV test is to calculate the speed of the *P* wave (Vp) to propagate within a specific distance in a solid specimen. The distance is determined between the transmitter and receiver of the UPV test device. While the distance is a fixed factor, the propagation time is a variable factor. It is influenced by several interrelated internal conditions, such as porosity, cracks-discontinuity, density, and modulus of elasticity of the solid specimen. Furthermore, the UPV test results indirectly describe the level of both the structural integrity and defects in the solid specimens.

Based on the observations of the available scientific literature, it was observed that UPV has been used as an effective and reliable method for the assessment of mechanical properties of solid materials such as rocks that are used in various geotechnical projects [43–45], cement-based materials like concrete [46–48], and mortar [49]. The UPV test has been used to develop several reliable relationships among experimentally obtained UPV wave data with various mechanical properties of fibrous concrete. For instance, the experimental results of UPV were further utilized by Ref. [50] in determining the modulus of elasticity and Poisson's ratio of fibrous concrete affecting the diverse properties of steel, polypropylene/polyethylene, and hybrid fibers.

A civil engineering project that specifically involves geotechnical engineers is the construction of embankments and revetments as slope stability work. In Indonesia, low slope protection is still constructed with mountain rocks or river stones with cement mortar as a binder and plaster owing to the huge mountain rocks and river stones, which are economically obtainable in large amounts in many regions. Hence, geotechnical engineers with knowledge regarding soil properties at the construction site should have an understanding of the performance of mortar as a binder and plastering. This is because it involves the strength and whole stability of the embankment or revetment construction. In addition, the mechanical properties of mortar (uniaxial compressive strength) have considerable control on the stability of central and peripheral rocks or stones in the revetment structures, such as embankments and slope protections that are constructed by composites of rocks and mortar. Hence, this study uses compressive strength as a method for investigating mortar.

In geotechnical and geological engineering environments, the point load strength index (PLSI) test is one of the main evaluation methods that is commonly used for determining the structural integrity of rock as a brittle material. In addition, point load strength (Is_{50}) obtained from the PLSI test is an important parameter of interest. Notably, several previous studies have explained that the geometric nature of the mechanical load of the point load test generates a failure mechanism, which similarly resembles a tensile failure, and indeed relates well with the indirect and direct tensile strength tests [21]. Accordingly, it is of interest that the stress and failure mechanism obtained from the PLSI test in this study may be regarded as a type of tensile strength test. Furthermore, the reliable PLSI value for predicting rock strength has attracted the interest of a number of researchers using the PLSI testing with the aim of studying the structural integrity of cement-based materials such as concrete in withstanding point loads [51,52]. Hence, the potential of the PLSI test in enriching the physical properties of cement-based materials such as cement mortar is the rationale behind this research in using the PLSI test as one of the procedures for investigating fibrous mortar. Moreover, the addition of fiber to the mortar or concrete mixture aims to increase the tensile capacity and toughness and limit the occurrence and propagation of cracks due to load. Previous studies by Refs. [53,54] showed that the suitability of the PLSI test in determining the tensile stress of solid materials, which may adapt to evaluate the contribution of fiber in increasing the tensile value of fibrous mortar.

This study considers the widespread use of mortar; however, knowledge of the mechanical behavior of plain mortar and fibrous mortar needs to be improved through experimental investigations including UPV, compressive strength, and PLSI tests. Cement mortar as a bonding and plastering material is vulnerable to various aggressive actions such as varying subjected loads, changes in temperatures and weather, and extreme environments. Regardless, effective testing and evaluation of the cement mortar mixture are of great importance; however, appropriate mortar can be produced as reliable and tough construction material against various aggressive actions. Accordingly, a combination of various testing methods rather than a single method would give more accurate information on the cement mortar used in this study, particularly when it is vulnerable to various subjected loads. In this study, attempts were made to elucidate the relationships among the UPV test, compressive strength test, and PLSI test results.

2. Research significance and novelty

Nowadays, carbon sheet fiber is a cutting-edge material that is widely used to improve structural element performance. But sometimes many deductions are unused. Apart from that, most research on short carbon fiber uses virgin fiber. While, the inclusion of SCF into cementitious system is a relatively new area of research, and the literature reports only a few studies on the effective utilization of SCF into mortar [11,35,36,42]. To date, study on the compressive strength to assess the performance of SCF mortar is still lacking, and there are no studies exploring the use of UPV and point loads tests on fibrous cement-based materials. Therefore, the research significant of the present study is to utilize the SCF (12 mm in length) originated from unused carbon fiber sheets at dosages of 0.5 %, 1 % and 1.5 % by cement weight and their performances is asses through UPV, point load and compressive strength tests. The novelty of this research is to provide comprehensive investigation on the characteristics of reinforced and not reinforced mortar with SCF through compression tests, point load tests and UPV. The relationship between each test result of the compression test, point load test and UPV is used to predict compressive strength based on UPV, and compressive strength based on PLI. In addition, the relationship between the test results is used to confirm the test results carried out on the mortar prepared in this research.

3. Materials and experimental program

3.1. Materials

Portland cement composite (PCC), a type of blended cement produced by a national cement factory, widely and economically available on the national market and in compliance with SNI 7064:2014 [55] and having a specific gravity of 3.05, was used as a cementitious material. The chemical compositions of PCC are listed in Table 1. Numerous studies have been performed as innovative steps to widely introduce the performances of blended cement in terms of PCC so that its usage is further enhanced. Research reports [56–59] demonstrate the performance advantages of PCC. River sand is used as fine aggregate with water absorption, fineness modulus, and specific gravity in surface saturated dry (SSD) of 1.6 %, 45 %, and 2.4, respectively. Fine aggregate is used under SSD conditions to make plain mortar and fibrous mortar.

The SCF with an average length of 12 mm (Fig. 1), derived from the unused strips of carbon fiber after strengthening or retrofitting structural elements, was used as an internal reinforcement for the mortar. The selected length of SCF was based on recommendations from previous researchers [34–36], where a carbon fiber length of 8–20 mm offered best mechanical and durability properties in cement-based materials. The aforementioned knowledge is the rationale to carefully utilize SCF in the amount of 0.5–1.5 % by weight of cement to produce fibrous mortar in the current research. The physical and mechanical properties of the SCF obtained from the manufacturer are presented in Table 2.

3.2. Mix proportion

The cement mortar made in this study is designed to achieve a compressive strength of 5.2 MPa at 28 days. This type of cement mortar is commonly used as a binder and plaster for stone masonry, river stones, and mountain rocks binders of short revetments, canals, and other constructions [60]. The ratio of the blended cement and sand is 1:2.75 while the water-cement ratio (w/c) of 0.63 was kept constant for each mixture. In addition, the SCF contained an amount of 0.5, 1, and 1.5 % by cement weight. Plain mortar, mortar containing 0.5, 1, and 1.5 % SCF are given identification marks, namely PL, SCF-0.5, SCF-1, and SCF-1.5, respectively. The mixed proportion of mortar is presented in Table 3.

Fig. 1. Physical appearance of SCF.

Table 2
Physical and mechanical properties of SCF.

Properties	Value
Modulus of elasticity, GPa	160
Tensile strength, MPa	2900
Elongation at break, %	1.8
Density, g/cm^3	1.6
Thickness, mm	1.2
Average length, mm	12

Table 3
Composition of a 1 m^3 mortar.

Mix ID	Water (kg)	Cement (kg)	Fine aggregate (kg)	Carbon fiber (kg)
PL	298	437	1300	0
SCF-0.5	298	437	1300	2.19
SCF-1	298	437	1300	4.37
SCF-1.5	298	437	1300	6.56

3.3. Sample preparation

Mortar mixing was done in several stages using a 2-L capacity mixer. The water and cement were mixed firstly for 30 s at a speed of 140 ± 5 revolutions per minute. Subsequently, sands were poured into the mixer and mixed at the same speed for 30 s and followed by adding the SCF to the mixture and mixing continued for 1 min at a speed of 285 ± 10 revolutions per minute. In addition, mixing was stopped; however, manual mixing was done for 30 s to allow ease of removal of mortar that was stuck to the lip and the top of the mixing bowl. Then, mixing continued for 60 s with a speed of 285 ± 10 revolutions per minute. All fresh plain and fibrous mortar were poured and molded into a 50 mm cube mold. All the produced mortar was covered with wet burlap and placed in the room for 24 h at room temperature and humidity of 25 °C and 65 RH, respectively. Furthermore, all the specimens were removed from the mold and preserved in water at 25 °C until the testing day.

Table 1
Oxides content of PCC.

Oxide	SiO2	Al2O3	Fe2O3	CaO	SO3	MgO	LOI	Others
Content, %	19.23	6.32	3.48	62.62	1.73	0.88	4.61	1.13

3.4. Testing methods

3.4.1. Fresh mortar

The effect of the addition of SCF on the mortar workability based on ASTM C1437 [61] was evaluated using the slump flow test. Further, visual observation was also conducted to identify the compatibility of SCF in the mortar mixture.

3.4.2. Ultrasonic pulse velocity (UPV)

In this study, experimental evaluation to determine the UPV value was undertaken at 7, 28, and 90 days. Pulse speed testing was conducted in a saturated surface dry condition based on the recommendation of ASTM C597 [62]. The UPV values of all mortar samples were obtained with a portable non-destructive digital indicator tester. According to the standard procedure [62], the use of ultrasonic pulses with a frequency of 54 kHz represents a wavelength of 6.4 mm, and it is recommended that the test object must have a minimum size of 32 mm. Hence, the 50 mm × 50 mm × 50 mm cube mortar sample used in this study complies with the [62] standard recommendations. The UPV value is obtained using Eq. (1).

$$V = L/t \tag{1}$$

where *V* is the speed of ultrasonic pulse velocity (m/s); L is the wavelength of the wave (m) and t is the travel time (s).

3.4.3. Point load strength index (PLSI)

The operated point load test meets the standards of ASTM D5731-16 [63] and is a reliable and flexible laboratory device used to date [64–67]. Loading is monitored and implemented analogously at a constant speed of 5 mm/s [52]. A set of computerized tools connected to a load cell and LVDTs were used simultaneously to measure the loading and the depth of penetration that occurred, respectively. At the elapsed time of 7, 28, and 90 days, point load tests were applied to the mortar specimens. The tests were conducted using widely available equipment that is reliable for testing rocks. To accurately establish the relationship between the point load value and the depth of penetration, a measurement of the applied point load and the associated depth of penetration were monitored and recorded continuously until the specimen failed. A load cell was used to accurately measure the applied point load. Two linear variable displacement transducers (LVDTs) were mounted vertically to measure the depth of penetration associated with the point loads. The average reading of the two LVDTs is defined as the penetration depth related to the applied point load. Load cells and LVDTs were coupled with a set of tools that record and monitor the ongoing activities. Fig. 2 shows the PLSI test tool in the form of a hydraulic compressor. Its frame is equipped with a load cell, and LVDTs are assembled with a set of data acquisition devices. Based on the recommendations stated in the ASTM D5731 [63] and point load stress (PLS), the value was calculated using the application of a point load to a lump mass, similar to a block sample that has an equivalent diameter (De). Equations (2) and (3) were used to obtain the PLS value (N/mm^2): P is the load (N), De is the effective diameter (mm), D is the diameter sample (mm), and W is the width of the sample. Furthermore, the point load strength index (Is_{50}) was determined at peak stress.

3.4.4. Compressive strength test

At the predetermined elapsed time of 7, 28, and 90 days, the mortar samples were subjected to the compressive strength test. Fig. 3 shows the device used to test the compressive strength of the mortar. To make a simple alignment between the PLSI test and the compressive strength of the mortar, a test was performed on the mortar sample using the same press machine used in the PLSI test. The loading rate was kept constant to be 0.01 in/min similar to the assumption of previous studies [52]. To maintain data accuracy, a load cell coupled with a set of data-capturing devices was used to monitor and record data during the compressive strength testing. The compressive strength value was calculated by dividing the peak load by the surface area of the mortar specimen.

Compressive strength testing at 7, 28, and 90 days allows for a comprehensive evaluation of concrete performance at various stages of its development. Since the compressive strength value is correlated with the fundamental properties of the mortar, therefore, it is crucial to test PLSI and UPV simultaneously with compressive strength because their correlation offers a thorough assessment of material performance.

4. Results and discussion

4.1. Fresh mortar

The observed flow values for plain mortar, and fibrous mortar containing 0.5, 1, and 1.5 % carbon fiber by weight of cement were 205, 171, 153, and 139 mm, respectively. Notably, the gradual addition of carbon fiber causes the flow value related to the level of workability in fresh conditions gradually decreased by 16.59, 25.37, and 32.20 % for SCF-0.5, SCF-1, and SCF-1.5, respectively, towards PL specimens. A similar trend was also reported in past studies [68], where the slump flow of mortar prepared with a 0.3 % addition of SCF decreased by 18.67 % compared to the control mortar. Furthermore, the workability of self-compacting concrete (SCC) reinforced with 0.25 %, 0.75 %, and 1.25 % SCF pieces was reduced by 3.31–11.5 % compared to SCC without SCF [69]. This reduction in workability is related to the fiber

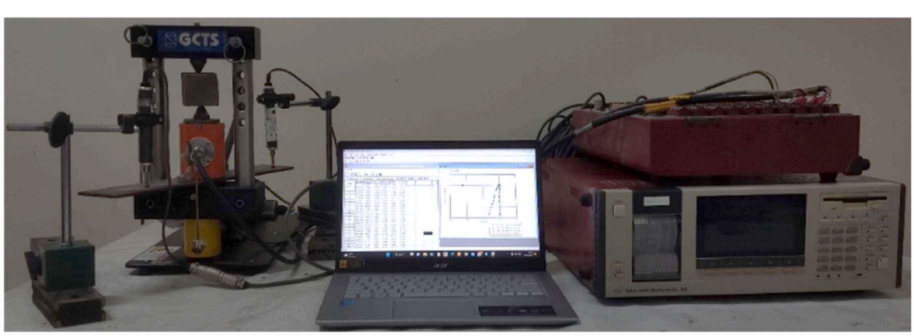

Fig. 2. Setup for PLSI test of mortar (cube specimen 50 mm × 50 mm × 50 mm).

$$\mathrm{PLS} = \frac{P}{De^2} \tag{2}$$

$$\mathrm{De} = \sqrt{4\mathrm{DW}/\pi} \tag{3}$$

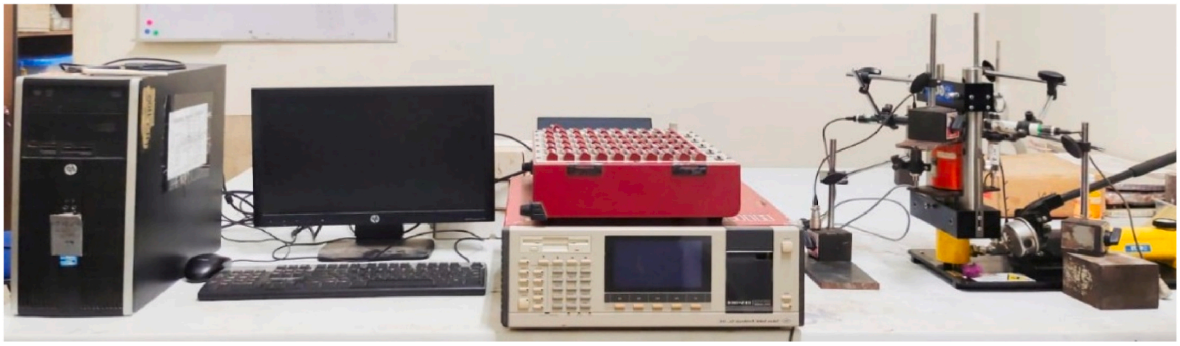

Fig. 3. Setup for compressive strength test of mortar (cube specimen 50 mm × 50 mm × 50 mm).

effect that occurred with the self-interlocking of SCF during the mixing process [70]. Furthermore, it is important to note that similar (or even worse) outcomes have been observed in the decreased workability of cementitious composites reinforced with different kinds of fiber. For instance, Chen et al. [71] showed that there was about 17.4 %, 24.8 %, and 39.1 % loss in slump flow for mortar prepared with 1 %, 2 %, and 4 % glass fiber, respectively, compared to control mortar.

As shown in Fig. 4, the fresh mortar did not segregate, in addition to bleeding and balling being absent in the fresh fibrous mortar. All forming materials including carbon fiber with a length of 12 mm were well-composed in each mixture of plain and fibrous mortar adopted in this study; therefore, it can produce fresh mortar with excellent performance. Accordingly, the excellent performance of the fresh mortar can enhance the ease of pouring and compaction.

4.2. UPV value

To evaluate the success level of placement and consolidation, before conducting a non-destructive test of UPV, destructive test (PLSI), and compressive strength, observations were made on the surface of all the hardened mortar specimens conducted. It can be seen that all the specimens have no paste loss and hairline shrinkage cracks on the surface (Fig. 5); thus, indicating that the materials forming plain and fibrous mortar are very well proportioned to allow perfect placement and consolidation.

Fig. 6 was prepared as quantitative evidence that measurably reports the UPV value of plain and fibrous mortar at each elapsed time of 7, 28, and 90 days. The investigation results showed that the UPV values of the plain mortar at the elapsed time of 7, 28, and 90 days obtained were 2702, 3074, and 3380 m/s, respectively. In reference to Fig. 6, it can be seen that at elapsed 7 days, the percentage increase in UPV value owing to the use of 0.5, 1, and 1.5 % short carbon fiber is 5.03, 7.95, and 9.10 %, respectively, as compared to the plain mortar specimens. At elapsed 28 days, the percentage increase in UPV value owing to the use of 0.5, 1, and 1.5 % short carbon fiber is 2.97, 4.82, and 9.74 %, respectively, as compared to plain mortar specimens. At elapsed 90 days, the percentage increase in UPV value owing to the use of 0.5, 1.0, and 1.5 % carbon fiber is 2.77, 5.49, and 10.68 % respectively, as compared to plain mortar specimens. Furthermore, the UPV value of fibrous mortar outperforms the plain mortar counterparts for all elapsed times. This evidence is the first part of prominent evidence observed from UPV testing on plain and fibrous mortar. The second prominent finding can be drawn by observing the effect of elapsed time on the UPV value of plain and fibrous mortar as shown in Fig. 6. Hence, this provides evidence that the UPV value of plain mortar blended cement increases with the elapsed time. The elapsed time facilitates an increase in UPV values of fibrous mortar blended cement. Observation of the first and second experimental findings clearly shows that the elapsed time along with the addition of fibers from 0.5 to 1.5 % simultaneously contributed to the gradual increase in UPV values.

Furthermore, the obtained experimental evidence can be reasonably elaborated as follows: in general. the porosity value decreases with the progress of hydration that occurs with the elapsed time that causes the cement paste to properly harden [72]. Considering that the blended cement behaves similarly to ordinary Portland cement (OPC), the adequacy of the mixed cement in the mortar mixture provides hydration progress which results in a good bond between the hydration products and the fine aggregate that forms a hardened plain mortar. A favorable porosity along the elapsed time [73], with the addition of carbon fiber, a good interface bond between the blended cement mortar and the carbon fiber can be obtained. The micro-sized fibers can serve as a filler, in combination with the unhydrated cement particles that can properly fill the voids left by the evaporated water in the hardened mortar, resulting in a carbon fiber-reinforced cement mortar with favorable porosity.

The obtained experimental evidence logically correlates with numerous findings in the available literature references that concern the value of wave propagation sensitive to porosity present in solid materials, such as rock [74]; cement-based materials, such as concrete [75]; cemented-paste backfill mortar [76], amongst others. At all elapsed times, it is clearly seen that the UPV values also incrementally improve

Fig. 4. Slump flow of fresh mortar (a) PL, (b) SCF-0.5, (c) SCF-1, and (d) SCF-1.5.

Fig. 5. Surface appearance of hardened mortar PL, SCF-0.5, SCF-1, and SCF-1.5 (left to right).

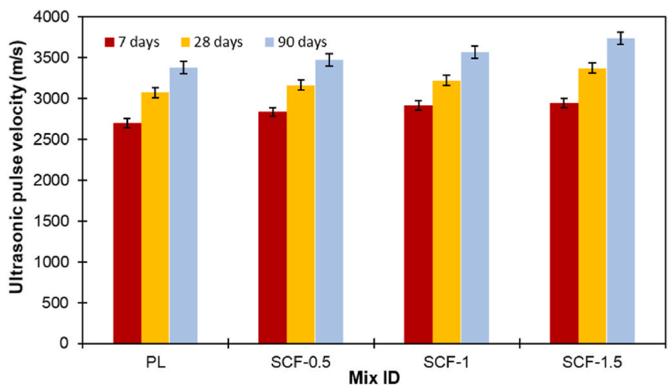

Fig. 6. UPV value of mortar specimen with different carbon fiber content and elapsed time.

as the use of fiber increases from 0.5 to 1.5 %. One possible interpretation of this experimental finding is that the ultrasonic pulse propagation finds no apparent internal flaws such as macro voids, fiber balling and macrocracks-discontinuity.

4.3. PLSI test

4.3.1. Point load stress (PLS) value-penetration depth curves

Fig. 7 is designed to illustrate the relationship between the point load value and penetration depth of plain mortar, and fiber mortar with carbon fiber contents of 0.5, 1, and 1.5 % of cement weight at elapsed times of 7, 28, and 90 days. The behavior of the plain and fibrous mortar under point load considering the effect of the elapsed time can be studied measurably through the relationship between Is_{50} and the cone penetration depth. Typical patterns of point load value-penetration depth curves are reported in Fig. 7. Based on a comparison of the curves, it was observed that all curves have a similar pattern with a linearity correlation between the point load value and the penetration depth up to the failure point; thus, indicating that the presence of carbon fiber has no effect on the brittleness of the mortar under point load.

In addition, the observations made on the influence of elapsed time on the point load value-penetration depth relationship of plain and fibrous mortar clearly indicate that the point load value-penetration depth response of all mortar mixtures is time dependent, irrespective of the fiber amount. Intrinsically, as expected, the elapsed time provides progress in the binder's hydration to harden the mortar. The elapsed time results in an increase in the point load value and an increase in the stiffness of the mortar, as evidenced by the slope between the point load value and the penetration depth, which becomes steeper as time elapses. The slope formed between the point load value and the penetration depth can be used to describe the level of stiffness of the mortar test object. Furthermore, it is observed that the slope in the plain mortar becomes steeper with the passage of time from 7 to 90 days, indicating that the stiffness of the plain mortar is increasing. In an advanced mortar, carbon fiber is gripped more tightly with increased stiffness. Furthermore, this resulted in greater structural integrity, leading to an increase in the point load value as observed in this study.

4.3.2. Is_{50} value

Fig. 8 shows the quantitative evidence of the peak of Is_{50} of plain mortar and its comparison to fibrous mortar with carbon fiber amounts of 0.5, 1, and 1.5 % by weight of cement at elapsed times of 7, 28, and 90 days. The results show that the Is_{50} of the plain mortar at the elapsed times of 7, 28, and 90 days are 0.36, 0.56, and 0.92 MPa, respectively. The hydration progress provides more hydration products as time elapsed, which improves the structural integrity of the hardened plain mortar to withstand a higher applied point load. According to Fig. 8, after 7 days, the percentage increase in Is_{50} value owing to the use of 0.5, 1.0, and 1.5 % carbon fiber is 16.33, 40.82, and 54.96 %, respectively, when compared to the plain mortar specimens. In addition, at elapsed 28 days, the percentage increase in Is_{50} value owing to the use of 0.5, 1.0, and 1.5 % carbon fiber is 50.97, 69.53, and 73.50 %, respectively, compared to the plain mortar specimens. Furthermore, at elapsed 90 days, the percentage increase in Is_{50} value owing to the use of 0.5, 1.0, and 1.5 % carbon fiber is 15.91, 26.52, and 30.30 % respectively, compared to the plain mortar specimens. Numerous studies have revealed that the point load applied to the test object can be categorized as a form of tensile loading that generates tensile stress on the test object; therefore, splitting occurs at failure [77]. The use of fiber will increase the ability to withstand cracking which in turn increases the tensile capacity of brittle specimens such as concrete. It is well established that during tensile loading, a sufficient amount of fibers facilitates the bridging action between cracks in the cement matrices, consequently reducing the crack growth rate [78]. In a similar mechanism, the increase of the carbon fiber content from 0.5 to 1.5 % by weight of cement in the blended cement-based mortar may provide a good bridging action that results in the superior Is_{50} value being obtained in the present investigation for the fibrous mortar compared to the plain mortar specimens.

4.3.3. Penetration depth

Fig. 9 shows the quantitative evidence of the peak penetration depth value of plain mortar, and its comparison to fibrous mortar with carbon fiber amounts of 0.5, 1, and 1.5 % by weight of cement at elapsed time of 7, 28, and 90 days. The results show that the penetration depths of the plain mortar at the elapsed time of 7, 28, and 90 days are 2.32, 3.07, and 3.11 mm, respectively.

According to Fig. 9, it can be noticed that at elapsed time of 7 days, the percentage increase in the penetration depth owing to the use of 0.5, 1.0, and 1.5 % carbon fiber is 25.65, 39.08, 52.33 %, respectively, compared to the plain mortar specimens. In addition, at elapsed time of 28 days, the percentage increase in penetration depth owing to the use of 0.5, 1.0, and 1.5 % carbon fiber is 3.82, 19.14, and 35.88 % respectively, compared to the plain mortar specimens. Furthermore, at an elapsed

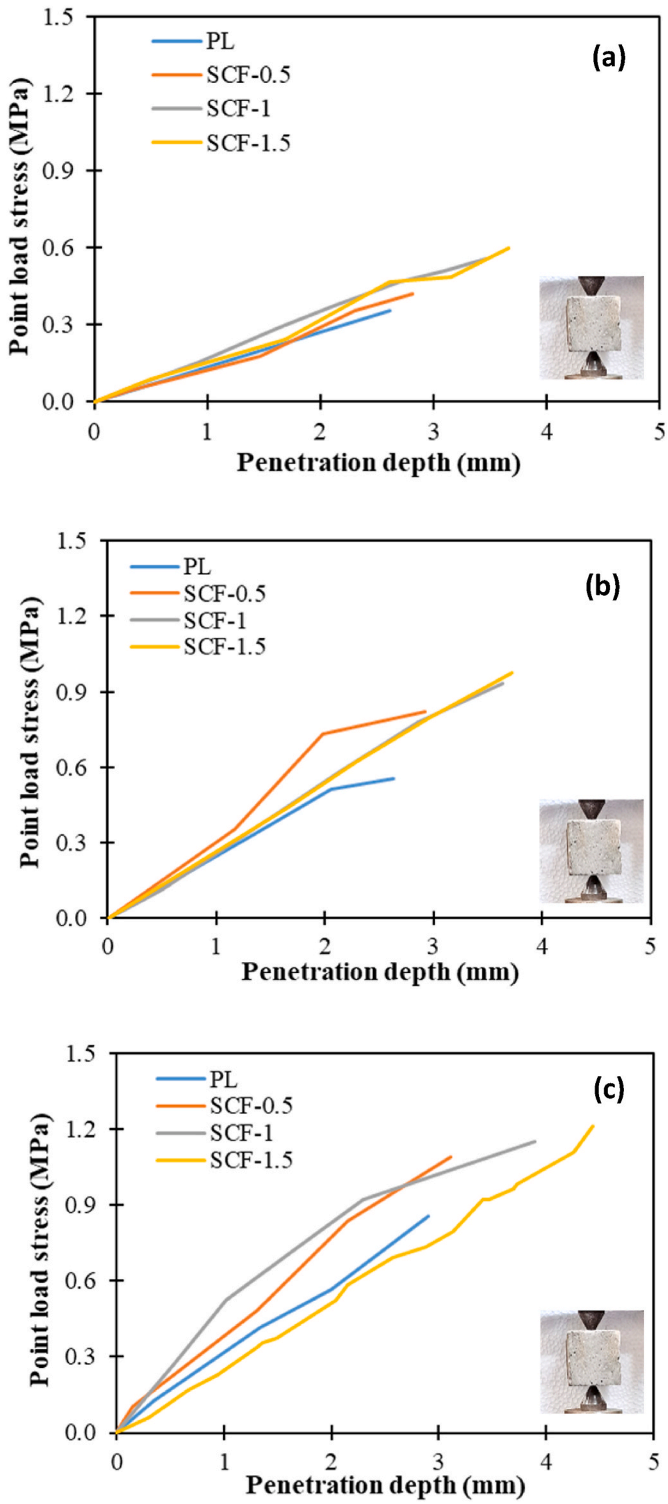

Fig. 7. Relationship between point load value and penetration depth of mortar specimens at different elapsed times: (a) 7 days; (b) 28 days and (c) 90 days.

time of 90 days, the percentage increase in penetration depth owing to the use of 0.5, 1.0, and 1.5 % carbon fiber is 2.98, 20.16, and 37.52 % respectively, compared to plain mortar specimens. Therefore, the results showed that there was an incremental improvement in the penetration depth value of fibrous mortar with the increment of carbon fiber amount from 0.5 % to 1.5 % by weight cement. As previously mentioned, this improvement in the penetration depth value resulted from the gradual use of carbon fiber from 0.5 to 1.5 % by cement weight, thus providing

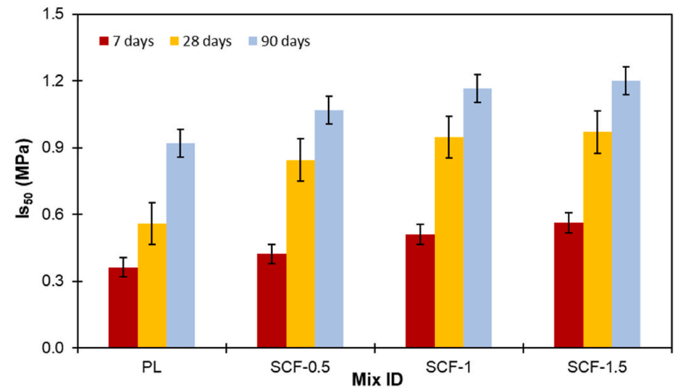

Fig. 8. Is_{50} value of mortar specimens at 7, 28, and 90 days.

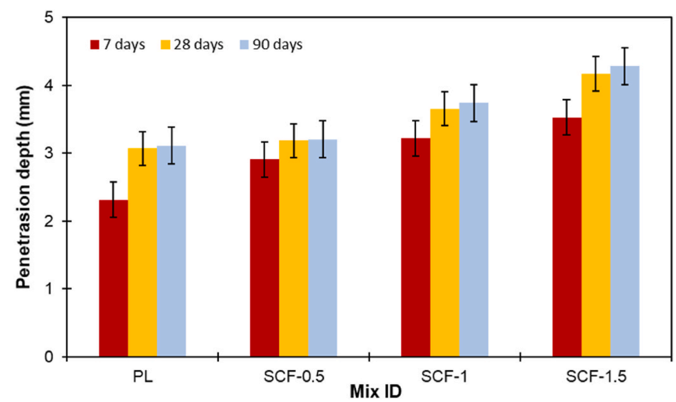

Fig. 9. Peak of penetration depth value of mortar specimens at 7, 28, and 90 days.

constant gradual improvement in the structural integrity of the materials. Furthermore, the cone of the PLSI test that penetrates the specimen creates a tensile mechanism within the specimen; therefore, fibrous mortar provides better resistance to crack opening and crack propagation than plain mortar, where failure occurs when the tensile stress exceeds the tensile stress limit of the carbon fiber. Because of the improvement in structural integrity, there is an inhibition in the point load failure process; therefore, it is required that the PLSI test cone penetrates deeper into the fibrous mortar, which is associated with the need for a higher Is_{50} value to obtain a failure state. Furthermore, mortar with weaker structural integrity only requires PLSI cones to penetrate the specimen shallowly and link the lower Is_{50} value that is needed to obtain a failure.

4.4. Compressive strength

Fig. 10 shows the quantitative evidence of the compressive strength of plain mortar, and its comparison to fibrous mortar with carbon fiber amounts of 0.5, 1, and 1.5 % by weight of cement at elapsed times of 7, 28, and 90 days. The results show that the compressive strengths of the plain mortar at the elapsed time of 7, 28, and 90 days are 3, 5.7, and 13.40 MPa, respectively. In the case of plain mortar, it is possible to presume that its behavior is strongly influenced by the hydration progress, where the porosity decreases with better microstructural changes owing to the hydration progress, as evidenced by the compressive strength of the hardened plain mortar which improves with the elapsed time.

Furthermore, the results show that, at elapsed time of 7 days, the percentage increase in compressive strength owing to the use of 0.5, 1.0, and 1.5 % carbon fiber is 39.33, 63.67, and 86.89 %, respectively,

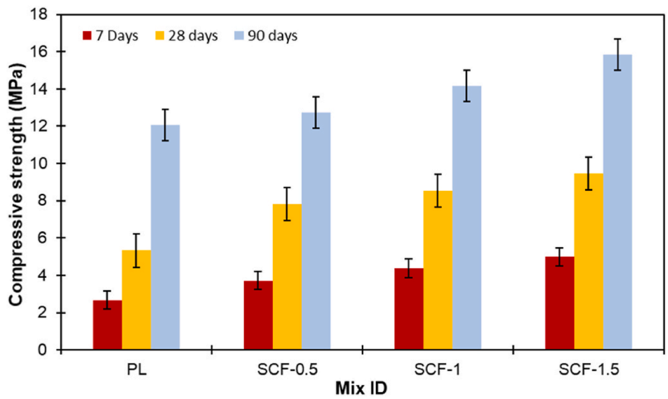

Fig. 10. Compressive strength of mortar with different carbon fiber contents at 7, 28, and 90 days.

compared to plain mortar specimens. At elapsed time of 28 days, the percentage increase in compressive strength owing to the use of 0.5, 1.0, and 1.5 % carbon fiber is 47.18, 60.34, and 78.01 %, respectively, as compared to the plain mortar specimens. At elapsed time of 90 days, the percentage increase in compressive strength owing to the use of 0.5, 1.0, and 1.5 % carbon fiber is 5.39, 17.23, and 31.15 %, respectively, as compared to the plain mortar specimens. A possible explanation for the compressive strength improvement in fibrous mortar is similar to the explanation of the influential factors that improve the PLSI value. The significance of carbon fiber in improving the compressive strength of fibrous mortar can be attributed to several interacting factors such as the uniform and randomly dispersed carbon fiber, the elapsed time, and the compatibility between the mechanical properties of carbon fiber and hydration products. During the hardening process, the hydration product grips firmly the carbon fiber to produce an excellent embedment; consequently, the fiber is excellently anchored so that it can function as reinforcement in the fibrous mortar. In addition, the carbon fiber contributes to an increase in compressive strength through the internal confining and bridging effect, which improves the structural integrity of fibrous mortar compared to its plain mortar counterpart. The results obtained in the present study are in line with previous research [79,80], where the addition of SCF increased the compressive strength of cement-based materials. The incorporation of SCF into cementitious composites increases their compressive strength by reducing crack propagation, enhancing bond resistance, and increasing energy absorption capabilities.

4.5. Failure pattern

Visual investigations were conducted on the specimens that had undergone PLSI and compressive strength testing. The failure patterns of the mortar under PLSI test at elapsed times of 7, 28, and 90 days are shown in Fig. 11. Detailed visual investigations showed that the failure pattern is characterized by splitting into two or three parts owing to the concentrated cracks path caused by the point load. These failure patterns are primarily responsible for the failure form of all specimens. Notably, two aspects can be drawn from the main failure pattern shown in Fig. 11. The first aspect is that, based on the main failure patterns that

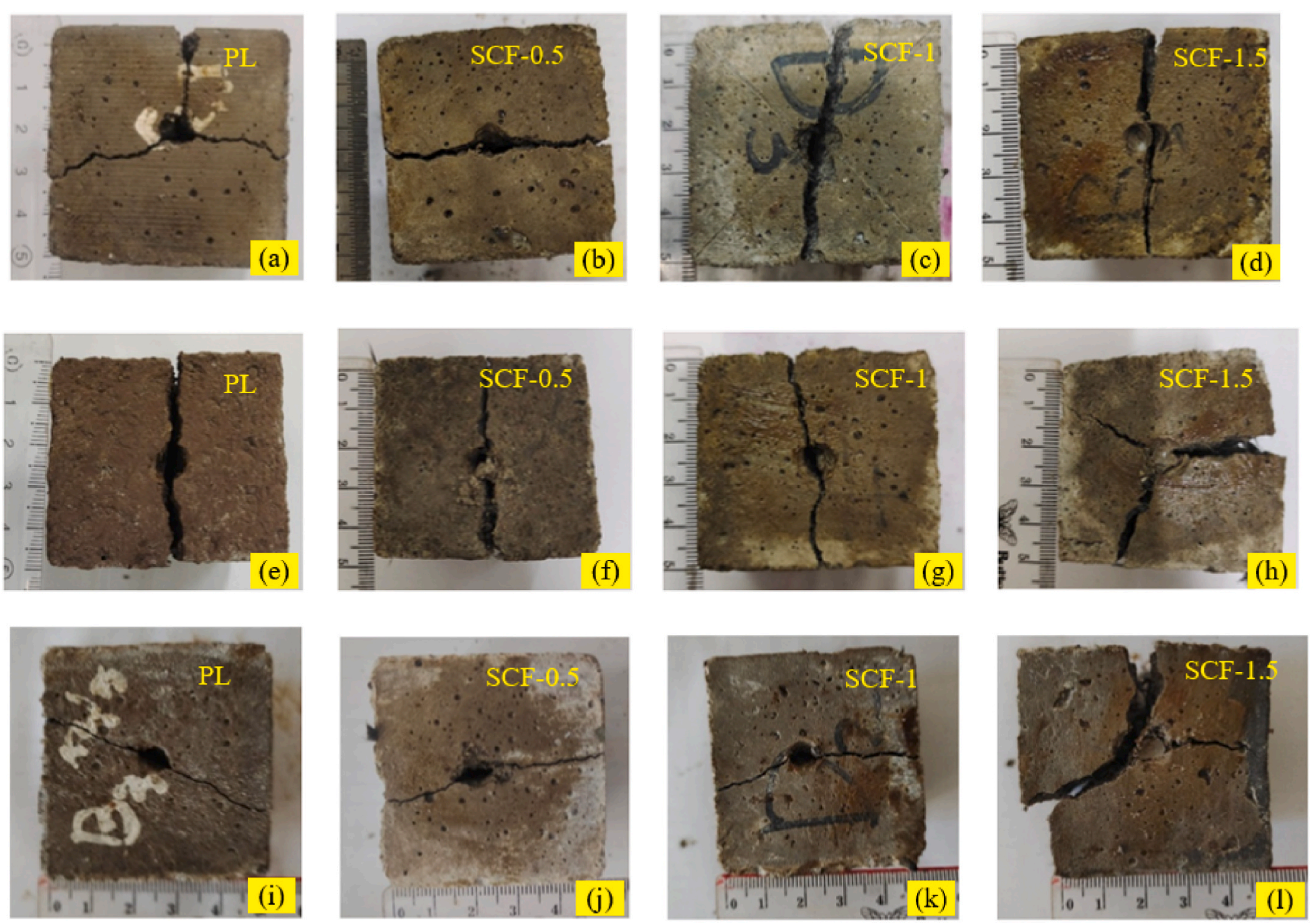

Fig. 11. Failure pattern of mortar under PLSI test at 7 days (a–d), 28 days (e–h), and 90 days (i–l).

occur on the test object, it can be established that the PLSI test has been performed correctly, as the ASTM D5731 [63] testing standard prescribes that the correct PLSI test will result in the solid specimens splitting into two or three parts. In addition, the nature of the failure patterns of the plain and fibrous mortar samples validates the correctness of the obtained experimental results. The second aspect that can be obtained from the visual observation of the main failure patterns that occurred and dominated the observed specimens is that the plain and fibrous mortar has sufficient structural integrity to sufficiently withstand the point load without breaking into pieces.

The failure patterns of the 50 mm cubical specimens under axial compressive load are shown in Fig. 12. The lateral expansion that emerges from the compressive load creates tensile stress that further contributes to crack propagation. Hence, as previously mentioned, the presence of fiber within a specified amount has at least two remarkable functions. The first function is the provision of a confining effect that impedes the lateral expansion while the second function is bridging across the developed cracks. Fig. 12 shows that two or three concentrated longitudinal macrocracks passed through the top of the cubical mortar specimens without multiple narrow longitudinal cracks. These experimental results establish that the addition of fiber did not alter the brittleness of both the plain mortar and fibrous mortar; hence, a similar

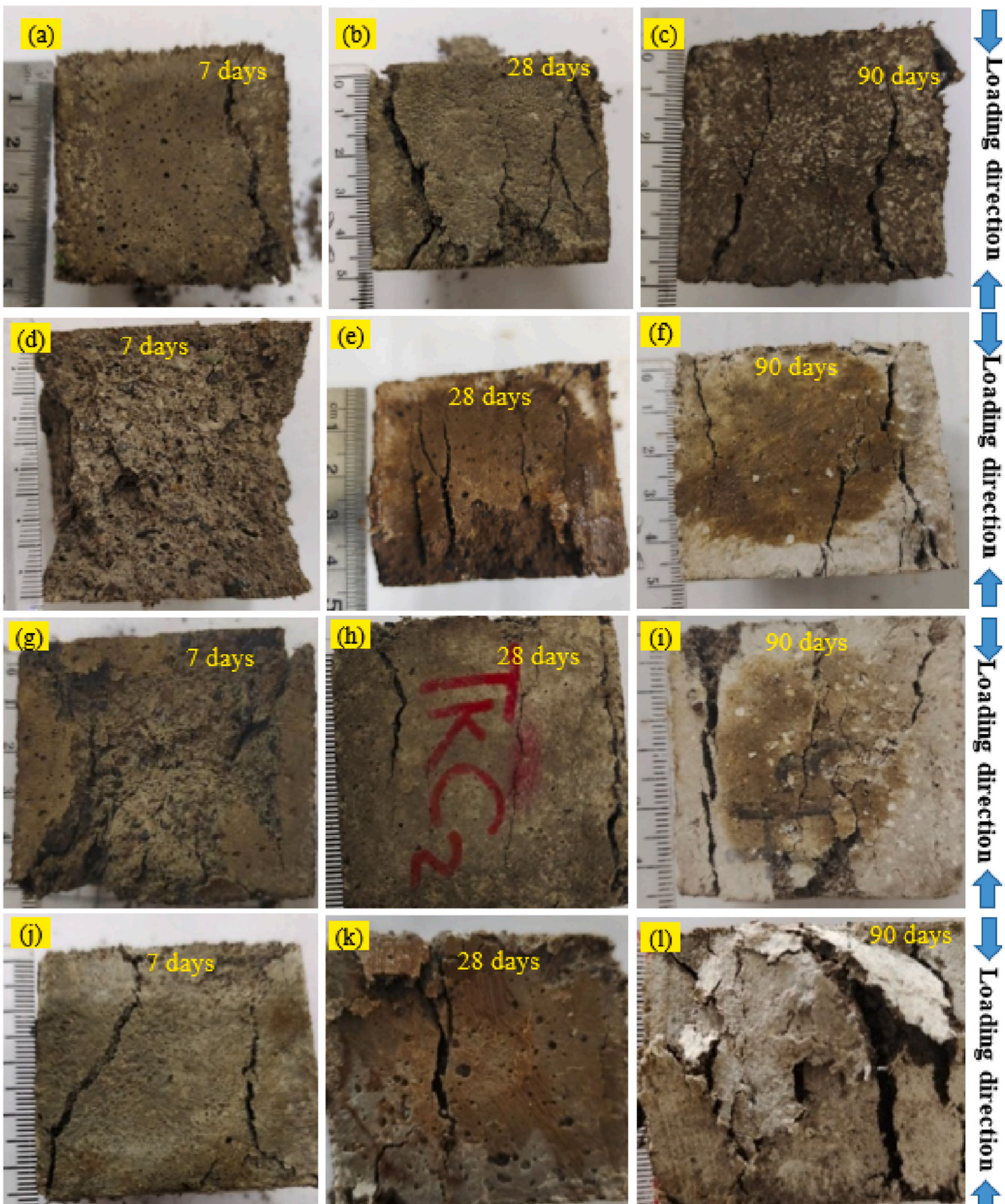

Fig. 12. Failure pattern of mortar specimen with different fiber content and elapsed time: (a) PL (a–c); (b) SCF-0.5 (d–f); (c) SCF-1 (g–i) and (d) SCF-1.5 (j–l).

failure pattern of all specimens owing to the compressive loads can develop. Furthermore, an explanation can be drawn that each mixture of the plain and fibrous mortar can be prepared and produced with a satisfactory level of uniformity, and along with the hydration progress, each mixture of hardened mortar has a homogeneous quality, which can be observed based on the similarity in the failure patterns.

The observed failure patterns in terms of the structural integrity of the mortar used in this study, as identified in the plain mortar, explain that the plain mortar maintains its form without breakage into pieces because of the good structural integrity of the hardened plain mortar. The use of carbon fiber in the range of 0.5–1.5 % by weight of cement to produce fibrous mortar results in all fibrous mortar having a failure pattern similar to that of the plain mortar. Hence, it can be confirmed that each mixture of hardened mortar provides a sufficient embedment of carbon fiber that improves the structural integrity in terms of both compressive and tensile strengths, which is reflected in the failure of the fibrous mortar without breakage into pieces even in higher applied compressive loads in comparison to the plain mortar.

4.6. Correlation between mechanical properties

In the current study, the commonly used regression analysis was applied to determine the trendline of the PLSI and compressive strength relationship. Several relationship trendline possibilities were studied, including logarithmic, linear, exponential, and power trendline. One of the advantages of combining PLSI and compressive strength testing is that the results can be used to estimate the tensile strength represented by the PLSI value that has a relationship to the compressive strength value or vice versa, where prediction of the compressive strength value can be made through the PLSI value. At the end of the trendline determination process the PLSI and compressive strength measurements for the prepared samples exemplify properly the linear equation with an R^2 value of 0.93, as shown in Fig. 13. The high R^2 of 0.93 provides an adequate approximation for comparing PLSI and compressive strength values. Previous research has revealed the relationship between PLSI and compressive strength expressed by a linear trendline [66,81,82]. The trend line from the results can be used as valuable information to mutually predict the accuracy of both the UPV and compressive strength results of mortar. This indicates that the relationship between the PLSI and compressive strength values can be used to predict the level of a mortar's ability to overcome the susceptibility to failure owing to the exceedance of either the compressive or tensile stresses, in which the tensile stress can be represented by the PLSI value.

Apart of that, the regression method is implemented to create a trendline for the relationship between UPV and compressive strength. A range of trend line alternatives were explored, including logarithmic, linear, exponential, and power curves. Following completion of the steps necessary to determine the approximate trendline of the relationship between UPV and compressive strength for the prepared samples, it is revealed that the relationship is adequately represented by an exponent trendline with an R^2 value of 0.96, as stated in Fig. 14. Each point represents the average of three compressive strength specimens with the same elapsed time and the same carbon fiber amount, where each compressive strength specimen was previously evaluated by the UPV test. The high R^2 of 0.96 provides an acceptable approximation when comparing UPV and compressive strength values. Previous study has shown that the relationship between compressive strength and UPV can be accurately represented by an exponential curve [83–85]. It resembles and almost coincides with the trend line formed from the formula established from other studies with high coefficient correlation (R^2 = 96.3 %); thus, confirming the correctness and reliability of the experimental method and results of the obtained UPV and compressive strength values. Furthermore, this study also informs the possibility of UPV indirectly measuring the compressive strength of mortar prepared with 50 mm cubes.

5. Conclusions

The following conclusions are drawn based on the experimental investigation findings that relate to specific materials and laboratory circumstances.

1. All mortar prepared with SCF had lower workability than the control mixture due to the fiber effect. However, all SCF mortar mixtures produced good compactability.
2. The UPV test revealed that the addition of short carbon fiber from 0.5 to 1.5 % can synergize with the matrix, leave no defects, and support the continuity of the hardening process; thus, implying that fibrous mortar has a better UPV value than plain mortar.
3. The increase in the PLSI value and compressive strength of fibrous mortar is attributed to the fact that carbon fiber is a stronger material that has much greater stiffness than the cement matrix; therefore, providing a confinement action that led to an increase in the structural integrity of fibrous mortar compared to that of plain mortar.
4. The correlation between the UPV value and compressive strength is similar to existing patterns with R^2 value of 0.93, thus validating the correctness and reliability of the results obtained in this study. Therefore, the UPV value can be used to predict the compressive strength value of mortar.
5. The correlation pattern that appears between the PLSI value and the compressive strength agrees with the results of existing patterns with R^2 value of 0.96. It further establishes the correctness and reliability

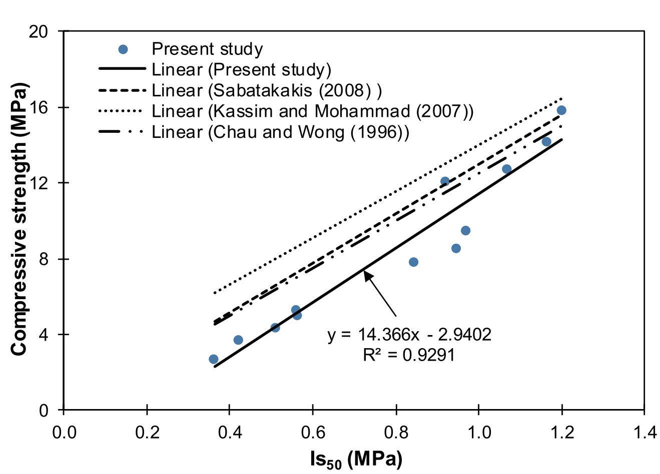

Fig. 13. Correlation between compressive strength and Is_{50}.

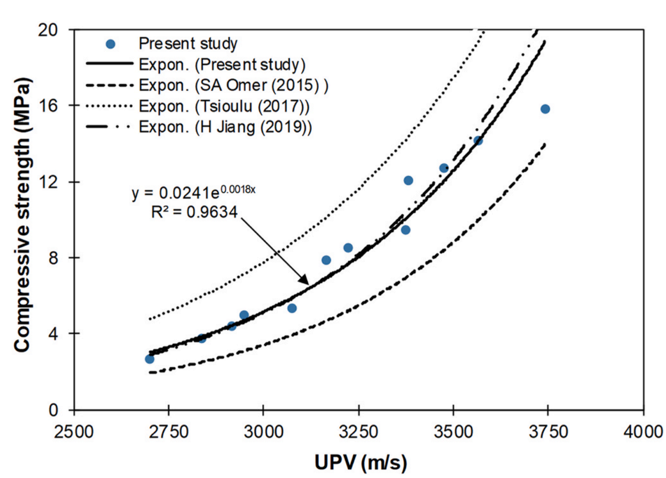

Fig. 14. Correlation between compressive strength and UPV.

of the results obtained in this study. Therefore, it may be used to estimate the threshold value of compressive strength based on the PLSI value and vice versa.

CRediT authorship contribution statement

Achmad Bakri Muhiddin: Conceptualization, Data curation, Formal analysis, Investigation, Methodology, Validation, Writing - original draft. **M.W. Tjaronge:** Conceptualization, Data curation, Formal analysis, Methodology, Validation, Visualization, Writing - review & editing. **Muhammad Akbar Caronge:** Formal analysis, Investigation, Methodology, Validation, Writing - review & editing. **Nur Hafizah A. Khalid:** Data curation, Formal analysis, Validation, Writing - review & editing.

Declaration of competing interest

The authors declare that they have no known competing financial interests or personal relationships that could have appeared to influence the work reported in this paper.

Data availability

Data will be made available on request.

References

[1] A. Danish, M.A. Mosaberpanah, M.U. Salim, M. Amran, R. Fediuk, T. Ozbakkaloglu, M.F. Rashid, Utilization of recycled carbon fiber reinforced polymer in cementitious composites: a critical review, J. Build. Eng. 53 (2022) 104583, https://doi.org/10.1016/J.JOBE.2022.104583.
[2] R. Napolitano, P. Vitale, C. Menna, D. Asprone, Development of sustainable perspective of carbon fibers recycling and reusing for construction materials, RILEM Bookseries 35 (2021) 131–142, https://doi.org/10.1007/978-3-030-76543-9_13/COVER.
[3] F. Meng, E.A. Olivetti, Y. Zhao, J.C. Chang, S.J. Pickering, J. McKechnie, Comparing life cycle energy and global warming potential of carbon fiber composite recycling technologies and waste management options, ACS Sustain. Chem. Eng. 6 (2018) 9854–9865, https://doi.org/10.1021/ACSSUSCHEMENG.8B01026/ASSET/IMAGES/MEDIUM/SC-2018-010264_0005.GIF.
[4] W.T. Lee, Y.J. Chiou, M.H. Shih, Reinforced concrete beam–column joint strengthened with carbon fiber reinforced polymer, Compos. Struct. 92 (2010) 48–60, https://doi.org/10.1016/J.COMPSTRUCT.2009.06.011.
[5] G.J. Ha, C.G. Cho, H.W. Kang, L. Feo, Seismic improvement of RC beam–column joints using hexagonal CFRP bars combined with CFRP sheets, Compos. Struct. 95 (2013) 464–470, https://doi.org/10.1016/J.COMPSTRUCT.2012.08.022.
[6] C.G. Karayannis, G.M. Sirkelis, Strengthening and rehabilitation of RC beam–column joints using carbon-FRP jacketing and epoxy resin injection, Earthq. Eng. Struct. Dynam. 37 (2008) 769–790, https://doi.org/10.1002/EQE.785.
[7] A.G. Tsonos, Effectiveness of CFRP-jackets and RC-jackets in post-earthquake and pre-earthquake retrofitting of beam–column subassemblages, Eng. Struct. 30 (2008) 777–793, https://doi.org/10.1016/J.ENGSTRUCT.2007.05.008.
[8] E. Esmaeeli, J.A.O. Barros, J. Sena-Cruz, L. Fasan, F.R. Li Prizzi, J. Melo, H. Varum, Retrofitting of interior RC beam–column joints using CFRP strengthened SHCC: cast-in-place solution, Compos. Struct. 122 (2015) 456–467, https://doi.org/10.1016/J.COMPSTRUCT.2014.12.012.
[9] A. Alrawashdeh, O. Eren, Mechanical and physical characterisation of steel fibre reinforced self-compacting concrete: different aspect ratios and volume fractions of fibres, Results in Engineering 13 (2022) 100335, https://doi.org/10.1016/J.RINENG.2022.100335.
[10] H.R. Pakravan, M. Latifi, M. Jamshidi, Hybrid short fiber reinforcement system in concrete: a review, Construct. Build. Mater. 142 (2017) 280–294, https://doi.org/10.1016/J.CONBUILDMAT.2017.03.059.
[11] F.F. Khorasani, M.Z. Kabir, Experimental study on the effectiveness of short fiber reinforced clay mortars and plasters on the mechanical behavior of adobe masonry walls, Case Stud. Constr. Mater. 16 (2022) e00918, https://doi.org/10.1016/J.CSCM.2022.E00918.
[12] T.R. Gyawali, Use of high ductile mortar mixing method for the enhancement of flexural fracture behaviour of steel filler mortar, Results in Engineering 18 (2023) 101096, https://doi.org/10.1016/J.RINENG.2023.101096.
[13] Q. Wang, Y. Zhou, M. Lai, M. Gu, J.C.M. Ho, Carbon fiber to improve the resistance of high strength PVA-ECC to elevated temperatures, J. Build. Eng. 71 (2023) 106475, https://doi.org/10.1016/J.JOBE.2023.106475.
[14] M. Nasir Uddin, L. zhi Li, A. Ahmed, K. Yahya Mohammed Almajhali, Prediction of PVA fiber effect in engineered composite cement (ECC) by artificial neural network (ANN), Mater. Today Proc. 65 (2022) 537–542, https://doi.org/10.1016/J.MATPR.2022.03.088.
[15] A.M. Tawfek, Z. Ge, H. Yuan, N. Zhang, H. Zhang, Y. Ling, Y. Guan, B. Šavija, Influence of fiber orientation on the mechanical responses of engineering cementitious composite (ECC) under various loading conditions, J. Build. Eng. 63 (2023) 105518, https://doi.org/10.1016/J.JOBE.2022.105518.
[16] Y. Wang, A.H. Kang, Z.G. Wu, P. Xiao, Y.F. Gong, H.F. Sun, Investigation of the basalt fiber type and content on performances of cement mortar and concrete, Construct. Build. Mater. 408 (2023) 133720, https://doi.org/10.1016/J.CONBUILDMAT.2023.133720.
[17] M. Yıldırım, H.B. Özhan, Durability properties of basalt fiber-reinforced mortars with different mineral admixtures exposed to high temperatures, Construct. Build. Mater. 400 (2023) 132574, https://doi.org/10.1016/J.CONBUILDMAT.2023.132574.
[18] Y. Li, Y. Su, K.H. Tan, X. Zheng, J. Sheng, Pore structure and splitting tensile strength of hybrid Basalt–Polypropylene fiber reinforced concrete subjected to carbonation, Construct. Build. Mater. 297 (2021) 123779, https://doi.org/10.1016/J.CONBUILDMAT.2021.123779.
[19] A. Mustea, D.L. Manea, Influence of polypropylene fibers upon the mechanical characteristics of reinforced composite mortars, Procedia Eng. 181 (2017) 338–345, https://doi.org/10.1016/J.PROENG.2017.02.398.
[20] A. Wygocka-Domagałło, H. Garbalińska, The effect of pore structure on the water sorption coefficient of cement mortars reinforced with 12 mm polypropylene fibres, Construct. Build. Mater. 248 (2020) 118606, https://doi.org/10.1016/J.CONBUILDMAT.2020.118606.
[21] Y. Guo, W. Li, W. Dong, Z. Luo, F. Qu, F. Yang, K. Wang, Self-sensing performance of cement-based sensor with carbon black and polypropylene fibre subjected to different loading conditions, J. Build. Eng. 59 (2022) 105003, https://doi.org/10.1016/J.JOBE.2022.105003.
[22] M. Mercuri, M. Vailati, A. Gregori, Lime-based mortar reinforced with randomly oriented polyvinyl-alcohol (PVA) fibers for strengthening historical masonry structures, Developments in the Built Environment 14 (2023) 100152, https://doi.org/10.1016/J.DIBE.2023.100152.
[23] Y. Zhang, Y. Zhang, R. Qian, G. Liu, H. Du, Influence of steel fiber on the water absorption of 3D printed concrete, Mater. Lett. 330 (2023) 133252, https://doi.org/10.1016/J.MATLET.2022.133252.
[24] G. Xiong, C. Wang, S. Zhou, Y. Zheng, Study on dispersion uniformity and performance improvement of steel fibre reinforced lightweight aggregate concrete by vibrational mixing, Case Stud. Constr. Mater. 16 (2022) e01093, https://doi.org/10.1016/J.CSCM.2022.E01093.
[25] B. Zhou, M. Zhang, L. Wang, G. Ma, Experimental study on mechanical property and microstructure of cement mortar reinforced with elaborately recycled GFRP fiber, Cem. Concr. Compos. 117 (2021) 103908, https://doi.org/10.1016/J.CEMCONCOMP.2020.103908.
[26] H. Rodin, S. Nassiri, K. Englund, O. Fakron, H. Li, Recycled glass fiber reinforced polymer composites incorporated in mortar for improved mechanical performance, Construct. Build. Mater. 187 (2018) 738–751, https://doi.org/10.1016/J.CONBUILDMAT.2018.07.169.
[27] B. Fu, K.C. Liu, J.F. Chen, J.G. Teng, Concrete reinforced with macro fibres recycled from waste GFRP, Construct. Build. Mater. 310 (2021) 125063, https://doi.org/10.1016/J.CONBUILDMAT.2021.125063.
[28] L. Li, B. Wang, M.H. Hubler, Carbon nanofibers (CNFs) dispersed in ultra-high performance concrete (UHPC): mechanical property, workability and permeability investigation, Cem. Concr. Compos. 131 (2022) 104592, https://doi.org/10.1016/J.CEMCONCOMP.2022.104592.
[29] H. Allam, F. Duplan, S. Amziane, Y. Burtschell, Assessment of manufacturing process efficiency in the dispersion of carbon fibers in smart concrete by measuring AC impedance, Cem. Concr. Compos. 127 (2022) 104394, https://doi.org/10.1016/J.CEMCONCOMP.2021.104394.
[30] H. Zhu, H. Zhou, H. Gou, Evaluation of carbon fiber dispersion in cement-based materials using mechanical properties, conductivity, mass variation coefficient, and microstructure, Construct. Build. Mater. 266 (2021) 120891, https://doi.org/10.1016/J.CONBUILDMAT.2020.120891.
[31] D. Zhang, J. Yu, H. Wu, B. Jaworska, B.R. Ellis, V.C. Li, Discontinuous micro-fibers as intrinsic reinforcement for ductile Engineered Cementitious Composites (ECC), Compos. B Eng. 184 (2020) 107741, https://doi.org/10.1016/J.COMPOSITESB.2020.107741.
[32] Fiber-Reinforced Cement Composites by Balaguru, N. Perumalsamy, Surendra P. Shah, in: Very Good Hardcover, first ed., Bradley Ross Books, n.d, 1992.
[33] A. Akbar, K.M. Liew, Assessing recycling potential of carbon fiber reinforced plastic waste in production of eco-efficient cement-based materials, J. Clean. Prod. 274 (2020) 123001, https://doi.org/10.1016/J.JCLEPRO.2020.123001.
[34] A. Saccani, S. Manzi, I. Lancellotti, L. Lipparini, Composites obtained by recycling carbon fibre/epoxy composite wastes in building materials, Construct. Build. Mater. 204 (2019) 296–302, https://doi.org/10.1016/J.CONBUILDMAT.2019.01.216.
[35] H. Nguyen, V. Carvelli, T. Fujii, K. Okubo, Cement mortar reinforced with reclaimed carbon fibres, CFRP waste or prepreg carbon waste, Construct. Build. Mater. 126 (2016) 321–331, https://doi.org/10.1016/J.CONBUILDMAT.2016.09.044.
[36] A. Belli, A. Mobili, T. Bellezze, F. Tittarelli, Commercial and recycled carbon/steel fibers for fiber-reinforced cement mortars with high electrical conductivity, Cem. Concr. Compos. 109 (2020) 103569, https://doi.org/10.1016/J.CEMCONCOMP.2020.103569.
[37] R.K. Graham, B. Huang, X. Shu, E.G. Burdette, Laboratory evaluation of tensile strength and energy absorbing properties of cement mortar reinforced with micro- and meso-sized carbon fibers, Construct. Build. Mater. 44 (2013) 751–756, https://doi.org/10.1016/J.CONBUILDMAT.2013.03.071.

[38] S.B. Park, B.I. Lee, Y.S. Lim, Experimental study on the engineering properties of carbon fiber reinforced cement composites, Cement Concr. Res. 21 (1991) 589–600, https://doi.org/10.1016/0008-8846(91)90110-4.

[39] H.A. Toutanji, T. El-Korchi, R.N. Katz, Strength and reliability of carbon-fiber-reinforced cement composites, Cem. Concr. Compos. 16 (1994) 15–21, https://doi.org/10.1016/0958-9465(94)90026-4.

[40] S. Akihama, T. Suenaga, T. Banno, Mechanical properties of carbon fibre reinforced cement composites, Int. J. Cem. Compos. Lightweight Concr. 8 (1986) 21–33, https://doi.org/10.1016/0262-5075(86)90021-7.

[41] P.W. Chen, D.D.L. Chung, Concrete reinforced with up to 0.2 vol% of short carbon fibres, Composites 24 (1993) 33–52, https://doi.org/10.1016/0010-4361(93)90261-6.

[42] A. Badanoiu, J. Holmgren, Cementitious composites reinforced with continuous carbon fibres for strengthening of concrete structures, Cem. Concr. Compos. 25 (2003) 387–394, https://doi.org/10.1016/S0958-9465(02)00054-9.

[43] K. Karaman, A. Kesimal, Correlation of schmidt rebound hardness with uniaxial compressive strength and P-wave velocity of rock materials, Arabian J. Sci. Eng. 40 (2015) 1897, https://doi.org/10.1007/S13369-014-1510-Z/METRICS. –1906.

[44] R. Fort, M. Alvarez de Buergo, E.M. Perez-Monserrat, Non-destructive testing for the assessment of granite decay in heritage structures compared to quarry stone, Int. J. Rock Mech. Min. Sci. 61 (2013) 296–305, https://doi.org/10.1016/J.IJRMMS.2012.12.048.

[45] M. Gomez-Heras, D. Benavente, C. Pla, J. Martinez-Martinez, R. Fort, V. Brotons, Ultrasonic pulse velocity as a way of improving uniaxial compressive strength estimations from Leeb hardness measurements, Construct. Build. Mater. 261 (2020) 119996, https://doi.org/10.1016/J.CONBUILDMAT.2020.119996.

[46] G. Trtnik, F. Kavčič, G. Turk, Prediction of concrete strength using ultrasonic pulse velocity and artificial neural networks, Ultrasonics 49 (2009) 53–60, https://doi.org/10.1016/J.ULTRAS.2008.05.001.

[47] N. Sabbağ, O. Uyanık, Prediction of reinforced concrete strength by ultrasonic velocities, J. Appl. Geophys. 141 (2017) 13–23, https://doi.org/10.1016/J.JAPPGEO.2017.04.005.

[48] K. Güçlüer, Investigation of the effects of aggregate textural properties on compressive strength (CS) and ultrasonic pulse velocity (UPV) of concrete, J. Build. Eng. 27 (2020) 100949, https://doi.org/10.1016/J.JOBE.2019.100949.

[49] C. Vipulanandan, V. Garas, Electrical resistivity, pulse velocity, and compressive properties of carbon fiber-reinforced cement mortar, J. Mater. Civ. Eng. 20 (2008) 93–101, https://doi.org/10.1061/(ASCE)0899-1561(2008)20:2(93).

[50] J. Carrillo, J. Ramirez, J. Lizarazo-Marriaga, Modulus of elasticity and Poisson's ratio of fiber-reinforced concrete in Colombia from ultrasonic pulse velocities, J. Build. Eng. 23 (2019) 18–26, https://doi.org/10.1016/J.JOBE.2019.01.016.

[51] H. Razzaghi, R. Madandoust, H. Aghabarati, Point-load test and UPV for compressive strength prediction of recycled coarse aggregate concrete via generalized GMDH-class neural network, Construct. Build. Mater. 276 (2021) 122143, https://doi.org/10.1016/J.CONBUILDMAT.2020.122143.

[52] R. Madandoust, Z.F.Z. Bazkiyaei, M. Kazemi, Factor influencing point load tests on concrete, Asian Journal of Civil Engineering 19 (2018) 937–947, https://doi.org/10.1007/S42107-018-0074-8/METRICS.

[53] K.T. Chau, X.X. Wei, A new analytic solution for the diametral point load strength test on finite solid circular cylinders, Int. J. Solid Struct. 38 (2001) 1459–1481, https://doi.org/10.1016/S0020-7683(00)00122-0.

[54] M.S. Al-Derbi, M.H. De Freitas, Use of the boussinesq equation for determining the distribution of stress within a diametrical point load test, Rock Mech. Rock Eng. 32 (1999) 257–265, https://doi.org/10.1007/S006030050047/METRICS.

[55] SNI 15-3500-1994, Portland Cement Composite, 1994. Indonesia National Standard (SNI).

[56] Y. Sunarno, M.W. Tjaronge, R. Irmawaty, Preliminary study on early compressive strength of foam concrete using Ordinary Portland Cement (OPC) and Portland Composite Cement (PCC), IOP Conf. Ser. Earth Environ. Sci. 419 (2020) 012033, https://doi.org/10.1088/1755-1315/419/1/012033.

[57] M.W. Tjaronge, R. Irmawaty, S.A. Adisasmita, A. Amiruddin, Hartini, Compressive strength and hydration process of self compacting concrete (SCC) mixed with sea water, marine sand and portland composite cement, Adv. Mater. Res. 935 (2014) 242–246, https://doi.org/10.4028/WWW.SCIENTIFIC.NET/AMR.935.242.

[58] A. Bhandari, S. Panthee, H. Atapour, A. Mortazavi, Point load test method for prediction strength of sustainable mortar made from blended cement and fly ash, IOP Conf. Ser. Earth Environ. Sci. 1117 (2022) 012029, https://doi.org/10.1088/1755-1315/1117/1/012029.

[59] M.A. Caronge, M.W. Tjaronge, H. Hamada, R. Irmawaty, Effect of water curing duration on strength behaviour of portland composite cement (PCC) mortar, IOP Conf. Ser. Mater. Sci. Eng. 271 (2017) 012018, https://doi.org/10.1088/1757-899X/271/1/012018.

[60] SNI 6882-2014, Standard Specification of Mortar for Masonry Application, Indonesian National Standard (SNI), 2014.

[61] Standard Test Method for Slump of Hydraulic-Cement Concrete , (n.d.). https://www.astm.org/c0143_c0143m-12.html (accessed January 14, 2023).

[62] Standard Test Method for Pulse Velocity Through Concrete , (n.d.). https://www.astm.org/c0597-16.html (accessed January 14, 2023).

[63] Standard Test Method for Determination of the Point Load Strength Index of Rock and Application to Rock Strength Classifications , (n.d.). https://www.astm.org/d5731-16.html (accessed January 14, 2023).

[64] M.E. Garrido, F.B. Petnga, V. Martínez-Ibáñez, J.B. Serón, C. Hidalgo-Signes, R. Tomás, Predicting the uniaxial compressive strength of a limestone exposed to high temperatures by point load and leeb rebound hardness testing, Rock Mech. Rock Eng. 55 (2022) 1–17, https://doi.org/10.1007/S00603-021-02647-0/FIGURES/11.

[65] A. Kayabaşı, C. Gökceoğlu, An assessment on the correlations between uniaxial compression strength and point load index, Arabian J. Geosci. (2022), https://doi.org/10.1007/S12517-021-09391-3, 15:3. 15 (2022) 1–13.

[66] W.Q. Xie, X.P. Zhang, Q.S. Liu, S.H. Tang, W.W. Li, Experimental investigation of rock strength using indentation test and point load test, Int. J. Rock Mech. Min. Sci. 139 (2021) 104647, https://doi.org/10.1016/J.IJRMMS.2021.104647.

[67] K.D. Chilton, Point load testing to more effectively measure bedrock strength, Nat. Rev. Earth Environ. (2021), https://doi.org/10.1038/s43017-021-00180-w, 2:7. 2 (2021) 449–449.

[68] C.A. Espinoza-Moreno, M. Rodriguez-Rodriguez, M.J. Pellegrini-Cervantes, C. P. Barrios-Durstewitz, R.E. Núñez-Jaquez, H.J. Peinado-Guevara, M. Chinchillas-Chinchillas, G. Fajardo-San-Miguel, Electrical percolation and fluidity of conductive recycled mortar cement: graphite powder: recycled sand with addition of industrial waste carbon fiber, Carbon Letters 31 (2021) 707–720, https://doi.org/10.1007/S42823-020-00188-0/METRICS.

[69] M. Mastali, A. Dalvand, The impact resistance and mechanical properties of self-compacting concrete reinforced with recycled CFRP pieces, Compos. B Eng. 92 (2016) 360–376, https://doi.org/10.1016/J.COMPOSITESB.2016.01.046.

[70] M. Mastali, Z. Abdollahnejad, A. Dalvand, A. Sattarifard, M. Illikainen, Comparative effects of using recycled CFRP and GFRP fibers on fresh- and hardened-state properties of self-compacting concretes: a review, New Materials in Civil Engineering (2020) 643–655, https://doi.org/10.1016/B978-0-12-818961-0.00019-3.

[71] X. Chen, H. Chen, W. Tan, Effect of glass powder on the mechanical and drying shrinkage of glass-fiber-reinforced cementitious composites, Case Stud. Constr. Mater. 17 (2022) e01587, https://doi.org/10.1016/J.CSCM.2022.E01587.

[72] L. Cui, J.H. Cahyadi, Permeability and pore structure of OPC paste, Cement Concr. Res. 31 (2001) 277–282, https://doi.org/10.1016/S0008-8846(00)00474-9.

[73] Z. Lafhaj, M. Goueygou, A. Djerbi, M. Kaczmarek, Correlation between porosity, permeability and ultrasonic parameters of mortar with variable water/cement ratio and water content, Cement Concr. Res. 36 (2006) 625–633, https://doi.org/10.1016/J.CEMCONRES.2005.11.009.

[74] A. Karakuş, M. Akatay, Determination of basic physical and mechanical properties of basaltic rocks from P-wave velocity , Http://Dx.Doi.Org/10.1080/10589759.2013.823606. 28 (2013) 342–353. https://doi.org/10.1080/10589759.2013.823606.

[75] T.U. Mohammed, M.N. Rahman, Effect of types of aggregate and sand-to-aggregate volume ratio on UPV in concrete, Construct. Build. Mater. 125 (2016) 832–841, https://doi.org/10.1016/J.CONBUILDMAT.2016.08.102.

[76] T. Yilmaz, B. Ercikdi, K. Karaman, G. Külekçi, Assessment of strength properties of cemented paste backfill by ultrasonic pulse velocity test, Ultrasonics 54 (2014) 1386–1394, https://doi.org/10.1016/J.ULTRAS.2014.02.012.

[77] K.T. Chau, R.H.C. Wong, Uniaxial compressive strength and point load strength of rocks, Int. J. Rock Mech. Min. Sci. Geomech. Abstracts 33 (1996) 183–188, https://doi.org/10.1016/0148-9062(95)00056-9.

[78] Y.M. Abbas, M. Iqbal Khan, Fiber–matrix interactions in fiber-reinforced concrete: a review, Arabian J. Sci. Eng. 41 (2016) 1183–1198, https://doi.org/10.1007/S13369-016-2099-1/METRICS.

[79] F. Grzymski, M. Musiał, T. Trapko, Mechanical properties of fibre reinforced concrete with recycled fibres, Construct. Build. Mater. 198 (2019) 323–331, https://doi.org/10.1016/J.CONBUILDMAT.2018.11.183.

[80] B. Han, L. Zhang, C. Zhang, Y. Wang, X. Yu, J. Ou, Reinforcement effect and mechanism of carbon fibers to mechanical and electrically conductive properties of cement-based materials, Construct. Build. Mater. 125 (2016) 479–489, https://doi.org/10.1016/J.CONBUILDMAT.2016.08.063.

[81] Z.M. Yusof, W.S. Farn, C.S. Leow, J.C. Lee, Rock point load test (PLT index) and its correlation with rock coring rate of bored pile machine, Phys. Chem. Earth, Parts A/B/C 129 (2023) 103344, https://doi.org/10.1016/J.PCE.2022.103344.

[82] N. Sabatakakis, G. Koukis, G. Tsiambaos, S. Papanakli, Index properties and strength variation controlled by microstructure for sedimentary rocks, Eng. Geol. 97 (2008) 80–90, https://doi.org/10.1016/J.ENGGEO.2007.12.004.

[83] S.A. Omer, R. Demirboga, W.H. Khushefati, Relationship between compressive strength and UPV of GGBFS based geopolymer mortars exposed to elevated temperatures, Construct. Build. Mater. 94 (2015) 189–195, https://doi.org/10.1016/J.CONBUILDMAT.2015.07.006.

[84] H. Jiang, J. Han, Y. Li, E. Yilmaz, Q. Sun, J. Liu, Relationship between ultrasonic pulse velocity and uniaxial compressive strength for cemented paste backfill with alkali-activated slag , Https://Doi.Org/10.1080/10589759.2019.1679140. 35 (2019) 359–377. https://doi.org/10.1080/10589759.2019.1679140.

[85] A.K. Saha, S. Majhi, P.K. Sarker, A. Mukherjee, A. Siddika, F. Aslani, Y. Zhuge, Non-destructive prediction of strength of concrete made by lightweight recycled aggregates and nickel slag, J. Build. Eng. 33 (2021) 101614, https://doi.org/10.1016/J.JOBE.2020.101614.